Electronic Supplementary Information

Simultaneous Preconcentration and Ultrasensitive On-site SERS Detection of Polycyclic Aromatic Hydrocarbons in Seawater Using Hexanethiol-modified Silver Decorated Graphene Nanomaterials

Shaojie Jia, [a, ‡] Dan Li,* [a, ‡] Essy Kouadio Fodjo,[b] Hu Xu, [a] Wei Deng, [a] Yue Wu [a] and Yuhong Wang * [a]

a Shanghai Institute of Technology, 100 Haiquan Road, Shanghai 201418, P. R. CHINA

b Laboratory of Physical Chemistry, University Felix Houphouet Boigny, 22 BP 582 Abidjan 22, Cote d'Ivoire

* **Corresponding Author**

E-mail: dany@sit.edu.cn

Content

SPE-SERS procedures

PAHs can be identified by the characteristic peaks in SERS spectra. A series of PAHs can be determined by using of hexanethiol-modified Ag NPs-decorated graphene nanocomposites (Ag/GN-SH). Moreover, Ag/GN-SH can be used as the adsorbents for solid-phase extraction (SPE) of PAHs. Specifically, the SPE cartridges were prepared by packing 100 mg of Ag/GN-SH in 3 mL empty SPE cartridges (Agilent) with an upper frit and a lower frit to avoid adsorbent loss, served as SERS-active substrates for detecting PAHs (toluene (TOL), naphthalene (NAP), anthracene (ANT), fluoranthene (FLU), pyrene (PYR) and perylene (PER)). Before each SERS measurement, the cartridges were loaded with 25 mL of the seawater sample solutions and the solutions were maintained

for 5 min, and eluted with 5 mL of 5 % (v/v) ethanol solution. The SERS spectra of PAHs on Ag/GN-SH were measured with a portable Raman system (BWTEK BWS415 *i*-Raman).

GC-MS analysis

GC-MS analysis was performed using an Rxi®-5Sil column (cross-linked 5% methyl phenyl silicone, 30 m x 0.25-mm i.d., 0.25-mm film thickness). The column oven temperature was initially held at 50 ^{o}C for 1 min, then programmed to reach 300 ^{o}C at a rate increase of 10 ^{o}C and held for 10 min. The total run time was 25 min. The temperatures of the injector port and the interface were set at 310 and 350 ^{o}C respectively. The carrier gas (helium) flow rate was 0.8 mL/min. The ionization energy was set at 70 eV. Mass spectra were collected by scanning from m/z 50 to m/z 550 at 2-s intervals.

Calculation of Enhancement Factors (EFs).

In order to calculate the SERS enhancement factors (*EFs*) of the silver electrodes used in this study, perylene (PER) is selected as a probe molecule for calculating the *EFs*. The *EFs* for PER can be calculated by the following formula: 1, 2

$$EFs = (I_{SERS}/I_{bulk}) \times (N_{bulk}/N_{surf})$$

where I_{SERS} and I_{bulk} are the intensities at the same band in the SERS and normal Raman spectrum of PER, respectively. N_{bulk} and N_{surf} are the number of molecules for the bulk sample and the number of molecules in the self-assembled monolayers (SAMs) absorbed on the Ag/GN-SH under laser illumination. The N_{surf} and N_{bulk} values can be calculated based on the estimation of the concentration of surface species or bulk sample and the corresponding sampling areas. 3 It is reported that the surface coverage of PER monolayer on Ag/GN-SH is considered to be Γ_{PER}=5.0 × 10^{13} molecules/cm^2 = 8.3× 10^{-11} mol/cm^2. 4 Taking the sampling area (ca. 1 μm in diameter) into account, N_{surf} has a value of 6.52×10^{-19} mol ($N_{surf} = \Gamma_{PER} \times \pi \times (1/2)^2$ μm^2 = 6.52×10^{-19} mol). For the bulk PER sample, the sampling volume is the product of the area of the laser spot (*ca.* 1 μm in diameter for 40× objective lens) and the penetration depth (~2 μm) of the focused laser beam. Assuming the density of PER is 1.286 g/cm^3, N_{bulk} can be calculated to be 8.00×10^{-15} mol (N_{bulk}=1.286 g/cm^3 × π × $(1/2)^2$ μm^2 × 2 μm / (252.3 g/mol) = 8.00×10^{-15} mol). For the vibrational mode at 1078

cm^{-1}, the ratio of I_{SERS} to I_{bulk} was about 10, hence *EF* was calculated to be 1.3×10^5. Similarly, the *EFs* for other PAHs can be calculated according to the former procedure. The *EFs* of characteristic vibrational modes of PAHs are shown in Table 1.

Adsorption Models

The Langmuir, Freundlich and Dubinin-Ashtakhov (DA) models were utilized to fit the adsorption isotherms of PAHs on Ag/GN-SH (Figure S8), respectively. 5, 6

The following expression describes the Langmuir equation:

$$Q_e = Q_m C_e/(K_L + C_e) \quad (1)$$

where Q_e (μg/mg) is the equilibrium-sorbed concentration, C_e (mg/L) is the equilibrium solution phase concentration, K_L (L/g) is the Langmuir constant, and Q_m (μg/mg) represents the maximum adsorption capacity of the adsorbent.

The following expression describes the Freundlich equation:

$$Q_e = K_F C_e^n \quad (2)$$

where K_F [(mg/g)/(mg/L)^n] is the Freundlich affinity coefficient, C_e (mg/L) is the equilibrium solution phase concentration, and *n* is the exponential coefficient.

The DA equation is as follows:

$$\log Q_e = \log Q_m + (\varepsilon_{sw}/E)^b \quad (3)$$

where $\varepsilon_{sw} = -RT\ln(C_e/C_s)$; ε_{sw} (kJ/mol) is the efficient adsorption potential; R [0.00831 kJ/(mol K)] and T (K) are the universal gas constant and the absolute temperature, respectively; C_e (mg/L) is the equilibrium solution phase concentration, Q_m (μg/mg) represents the maximum adsorption capacity of the adsorbent, C_s (mg/L) is the solute solubility in water; *E* (kJ/mol) is the "correlating devisor"; and b is the fitting parameter of the DA model.

The corresponding parameters calculated from the isotherms are summarized in Table S1 correspond very well to the DA model, which provides evidence that pore filling and flat surface adsorption is involved.

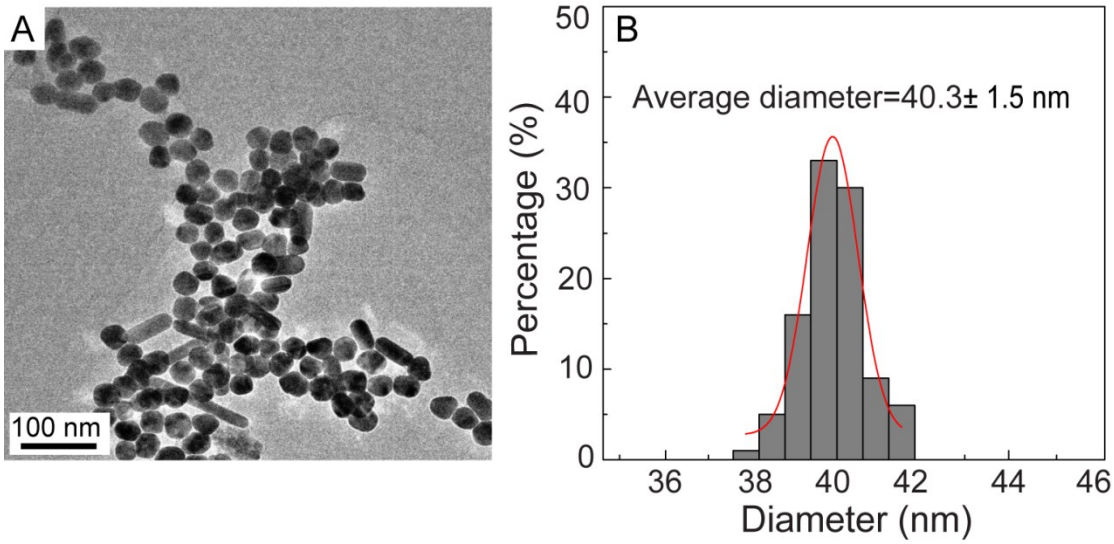

Fig. S1 (A) TEM image and (B) size distribution of Ag NPs.

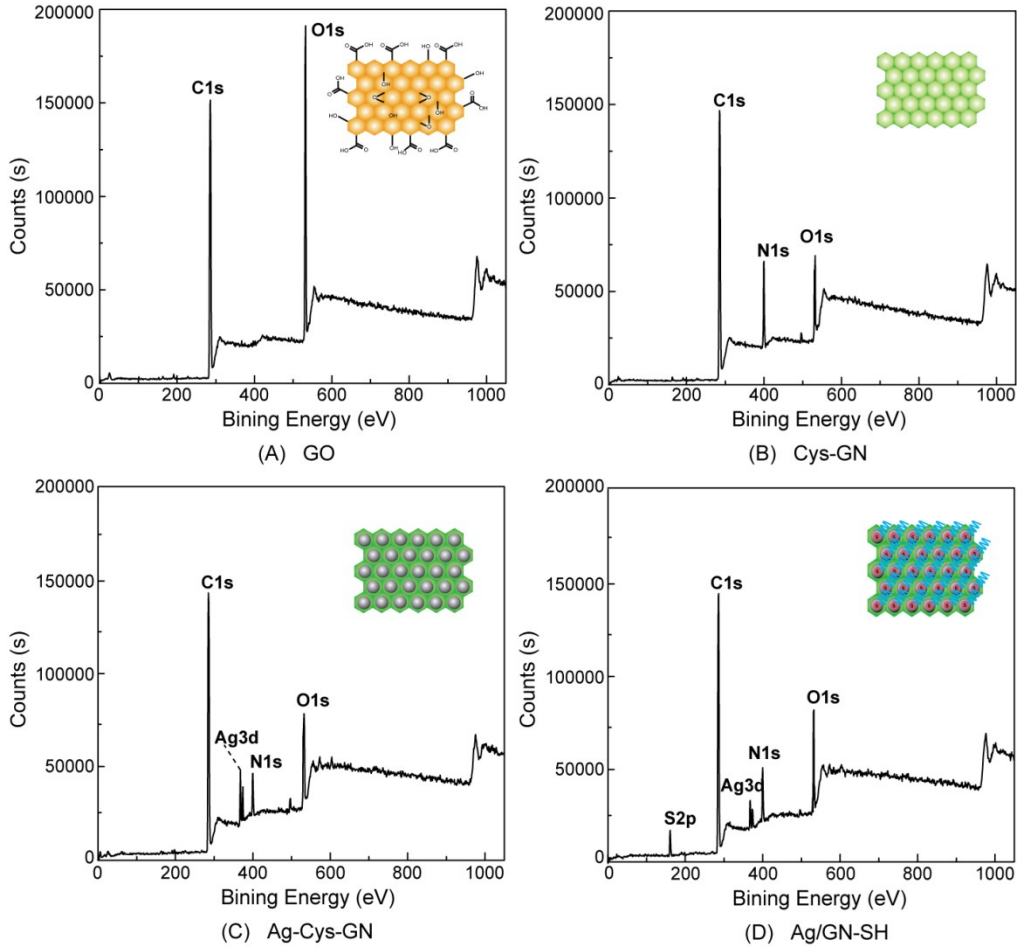

Fig. S2 XPS survey scans of (A) GO, (B) Cys-GN, (C) Ag-Cys-GN and (D) Ag/GN-SH.

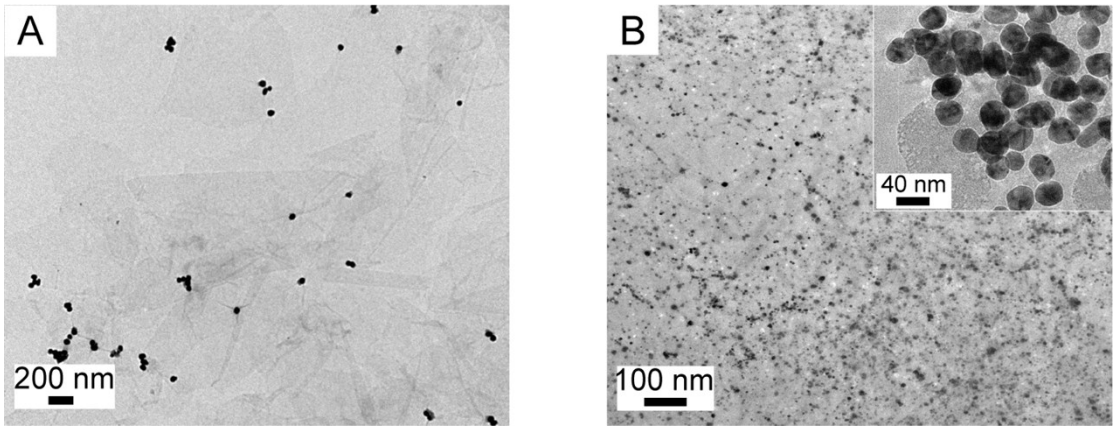

Fig. S3 Typical TEM images as-prepared (A) Ag-Cys-GN and (B) Ag/GN-SH. The upper right inset in (B) highlighting high-density Ag NPs are assembled on the surface of the Cys-GN.

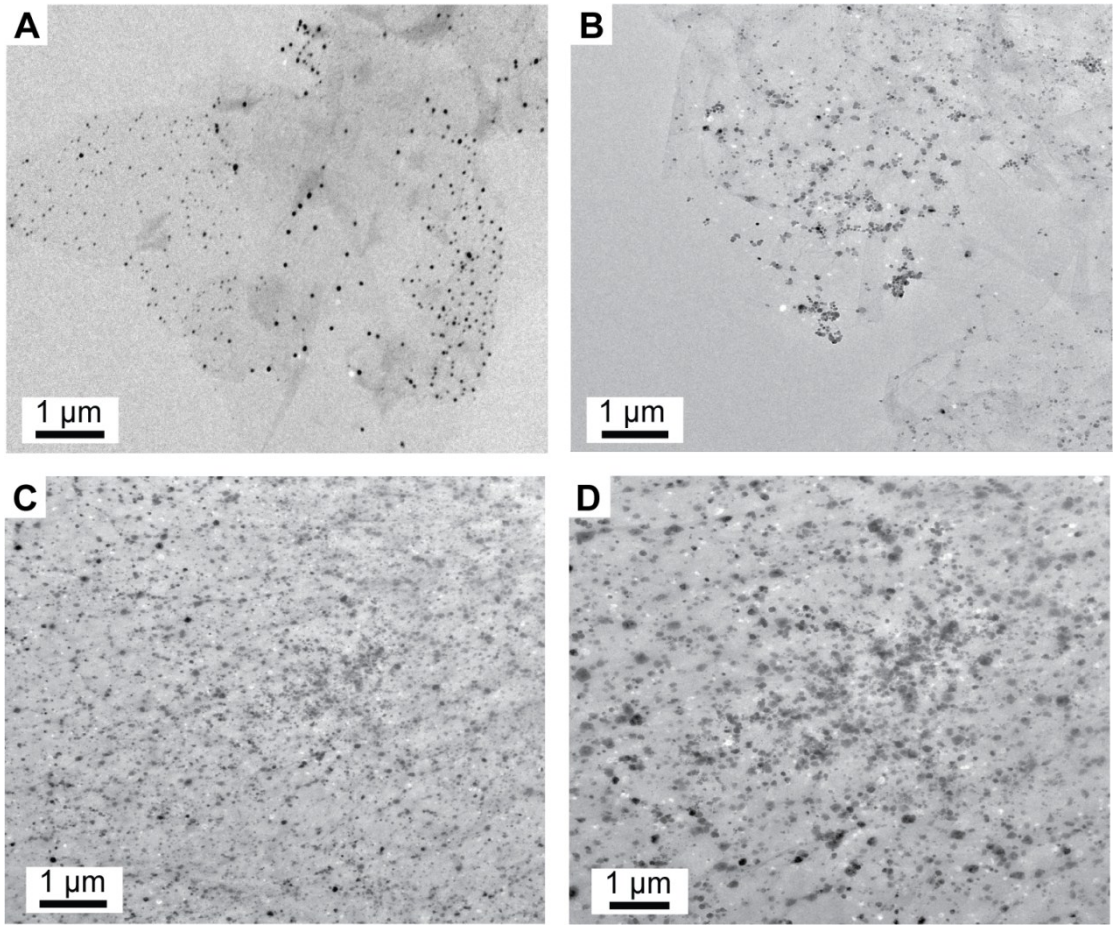

Fig. S4 TEM images of AgNP decorated Cys-GN (Ag-Cys-GN) with well-controlled densities of AgNPs. AgNP densities were varied by increasing the concentrations of Cys from (A) 1 mg/mL, (B) 5 mg/mL, (C) 10 mg/mL, (D) 20 mg/mL. The Cys-GN is prepared in the presence of 1 mg/mL GO and 10 mg/mL Cys. The diameter of Ag NPs has average diameters of 40 nm.

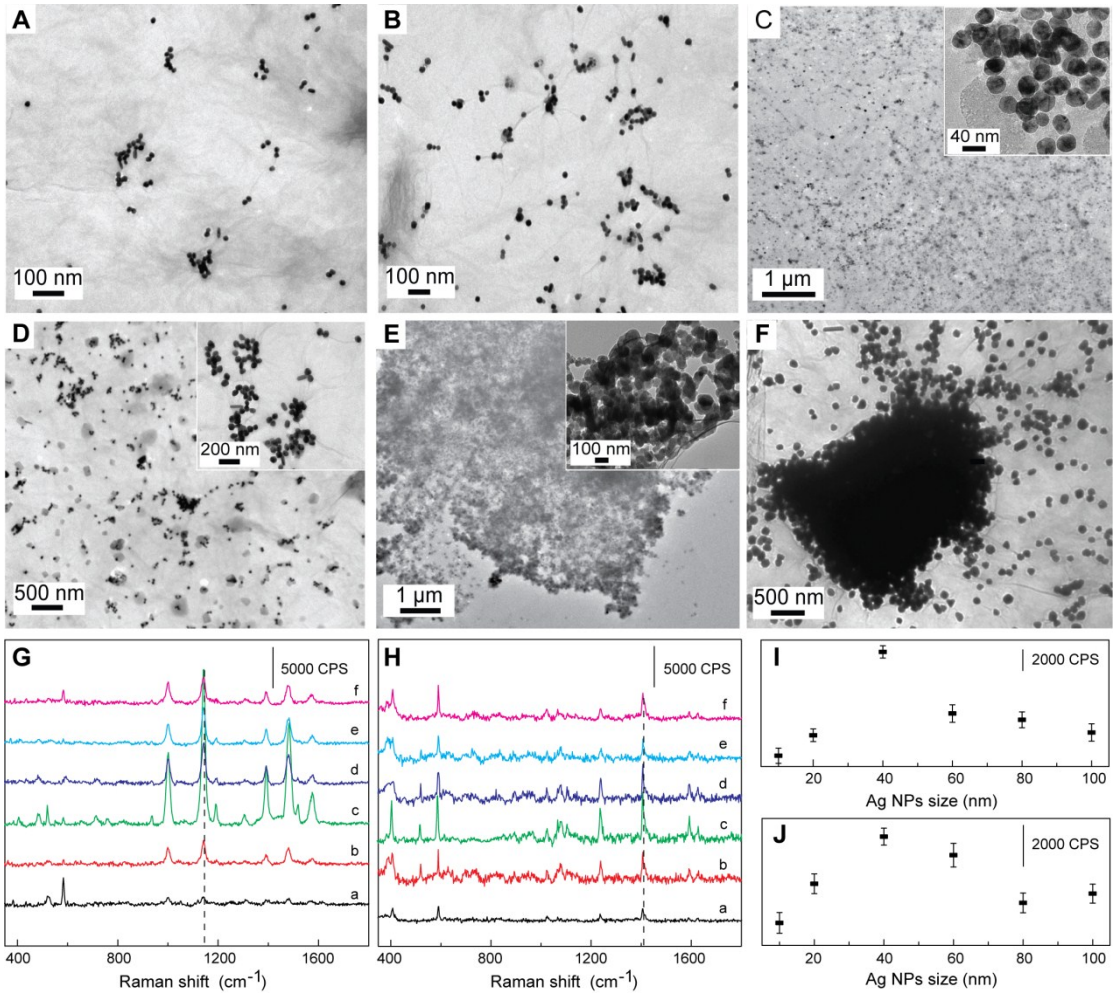

Fig. S5 TEM images of Ag/GN-SH decorated with Ag NPs that has different size: (A) 10 nm, (B) 20 nm, (C) 40 nm, (D) 60 nm, (E) 80 nm and (F) 100 nm. The Cys-GN is prepared in the presence of 10 mg/mL Cys, 1 mg/mL GO and 0.2 M SH. Inset of part (C–E): a magnified view. SERS spectra of Ag/GN-SH in 2×10^{-6} M ANT(G) and 2×10^{-6} M PYR (H) with different size of Ag NPs : a) 10 nm, b) 20 nm, c) 40 nm, d) 60 nm, e) 80 nm and f) 100 nm. The relationship between the intensity of 1143 cm^{-1} Raman band of ANT (I) and size of Ag NPs. The relationship between the intensity of 1407cm^{-1} Raman band of PYR (J) and size of Ag NPs. Each data point represents the average value from five SERS spectra on each sample. Error bars show the standard deviations associated with five measurements.

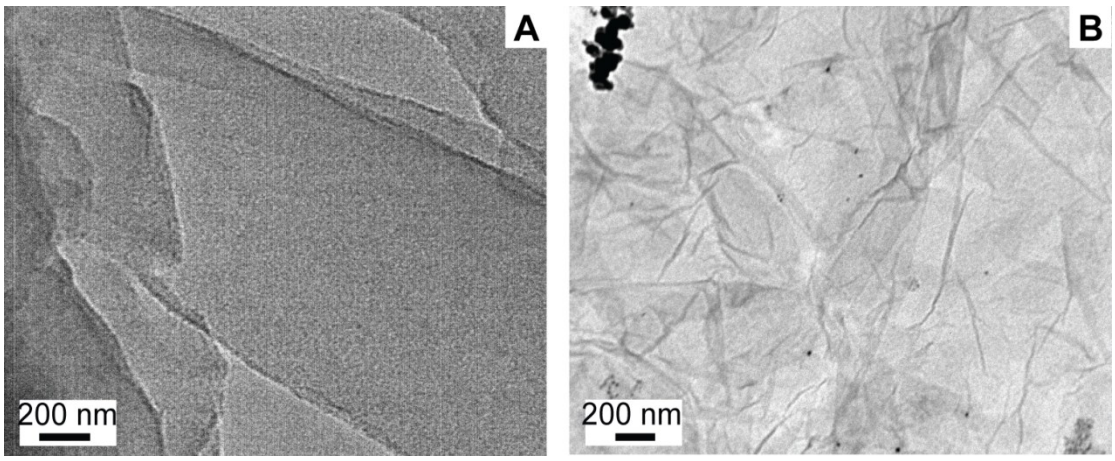

Fig. S6 Control experiments showing that Cys was critical for the assembly of Ag NPs on GO (left) and RGO (right) nanosheets. TEM images of (A) Ag NPs+GO and (B) Ag NPs+RGO in absence of Cys.

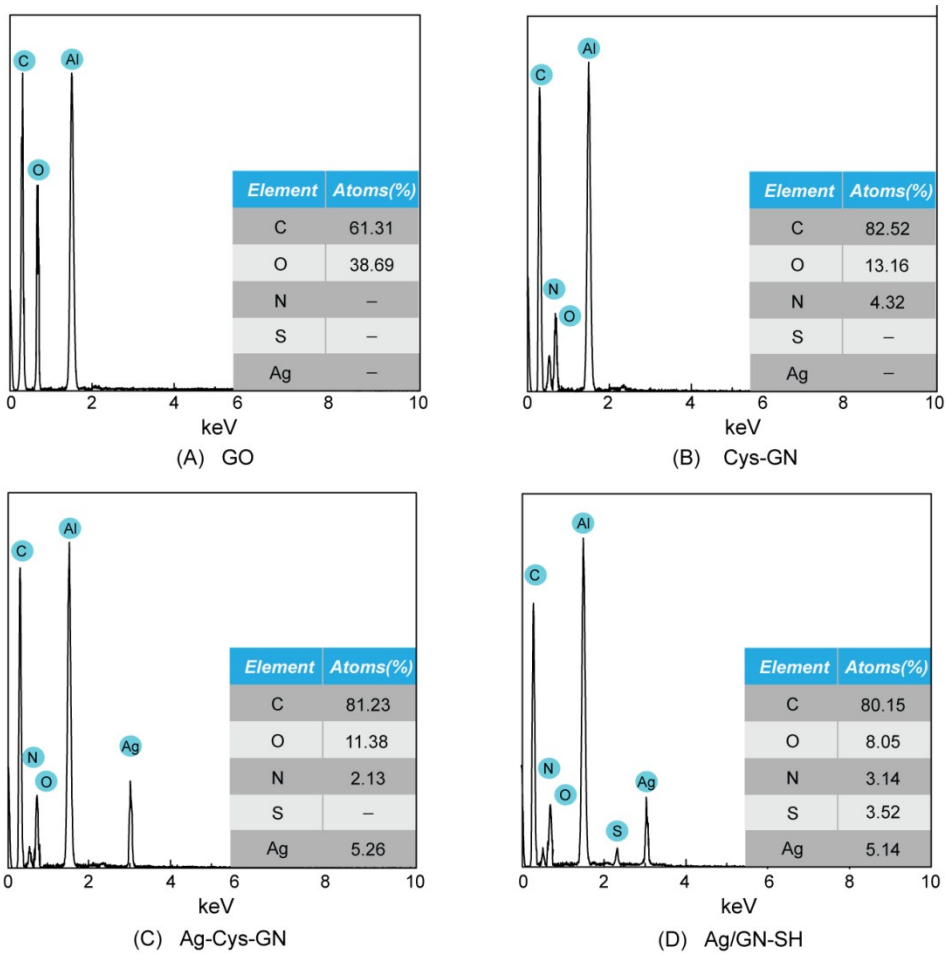

Fig. S7 EDS images of (A) GO, (B) Cys-GN, (C) Ag-Cys-GN and (D) Ag/GN-SH. The lower right inset in (A–D) is the elemental analysis results of corresponding nanomaterials.

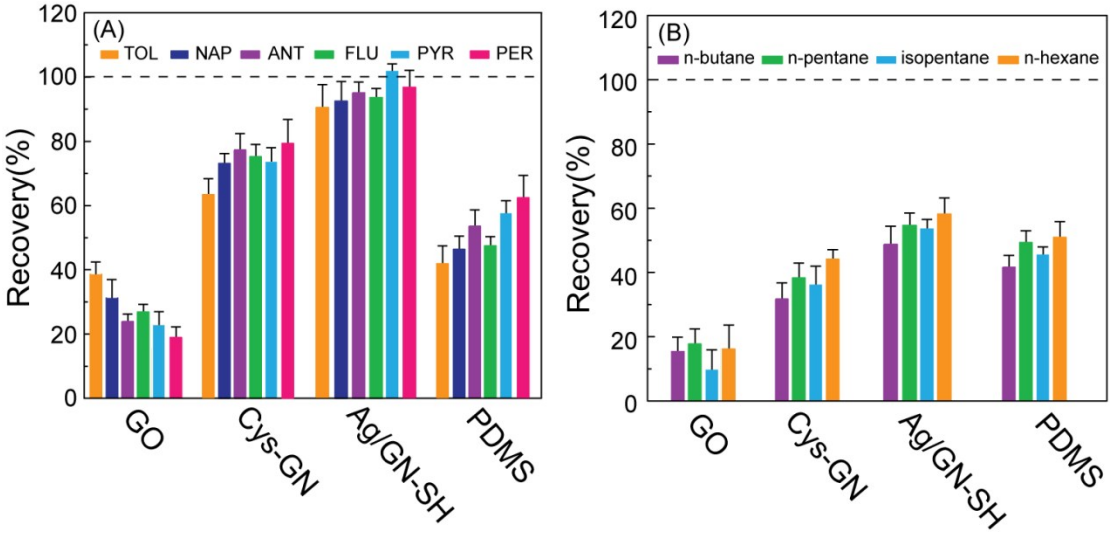

Fig. S8 Comparison of the adsorption performance of GO, Cys-GN, Ag/GN-SH and PDMS adsorbents for the SPE of aromatic compounds (A) and aliphatic compounds (B). GC-MS was used to quantify the amount of aromatic compounds and aliphatic compounds present.

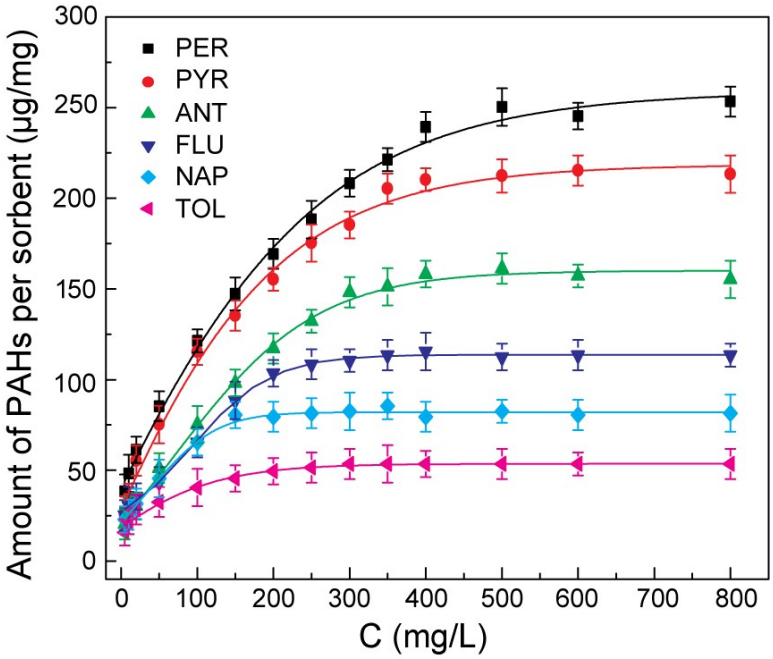

Fig. S9 Determination of the adsorption capacity of PAHs on Ag/GN-SH. 25 mL of PAHs solutions in different concentrations were passed through a SPE cartridge packed with 100 mg of Ag/GN-SH as adsorbent, and then the amount of adsorbed PCP was determined by GC-MS. The data were fitted to the Langmuir model. It showed that the saturated adsorption amount of PER for Ag/GN-SH was about 253.3 μg/mg, which was in the same order of magnitude with GN for adsorption of other PAHs compounds. 5, 6 Each data point represents the average value from five SERS spectra on each sample. Error bars show the standard deviations associated with five measurements.

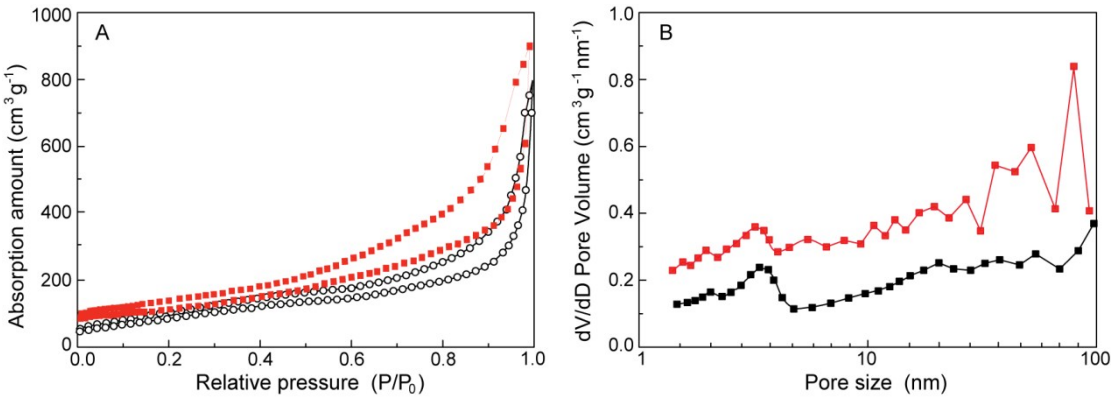

Fig. S10 (a) Nitrogen adsorption−desorption isotherms and (b) BJH adsorption pore size distribution of Ag/GN-SH and Cys-GN. (Ag/GN-SH, red line; Cys-GN, black line.)

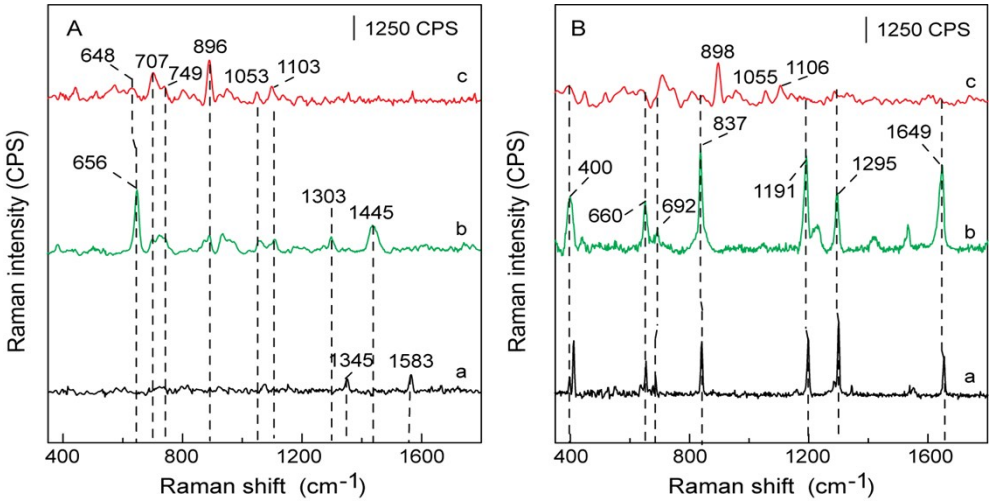

Fig. S11 (A) Raman spectrum of (a) Ag-Cys-GN, (b) SH and (c) Ag/GN-SH. (B) Raman spectrum of (a) methyl violet (MV); SERS spectrum of MV on (b) Ag-Cys-GN and (c) Ag/GN-SH. The concentration of MV is 1.0 mmol/L. The dotted lines indicate the representative vibration peaks of the analytes.

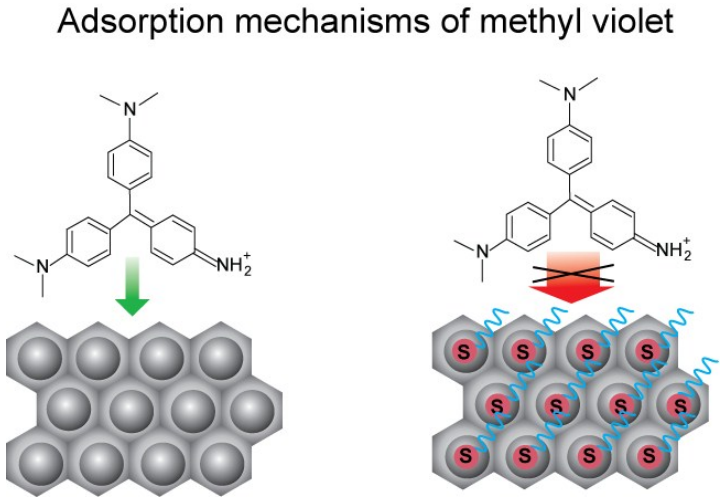

Fig. S12 Schematic representations of adsorption mechanism for MV.

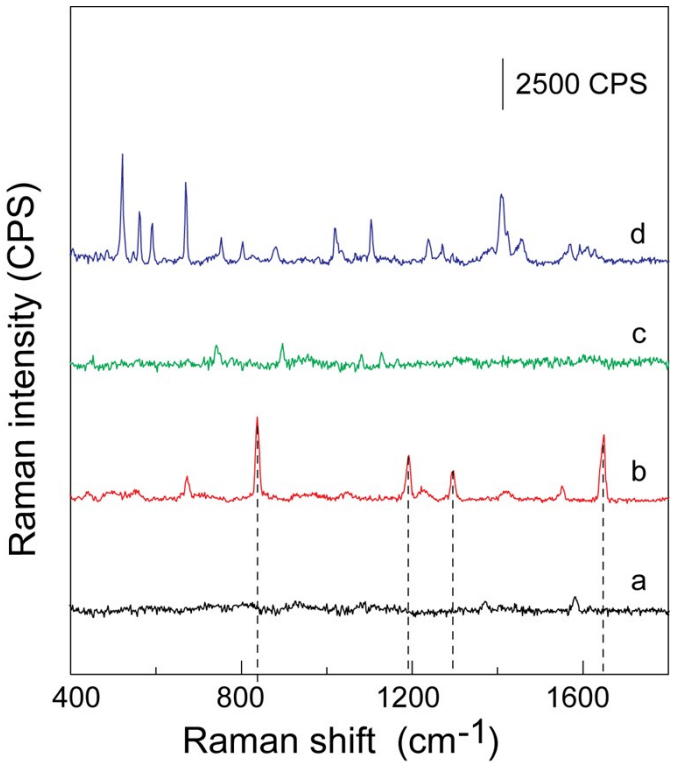

Fig. S13 Raman spectrum of Ag-Cys-GN (a) and Ag/GN-SH (c); SERS spectrum of MV and six PAHs on Ag-Cys-GN (b) and Ag/GN-SH (d). The dotted lines indicate the representative vibration peaks of MV.

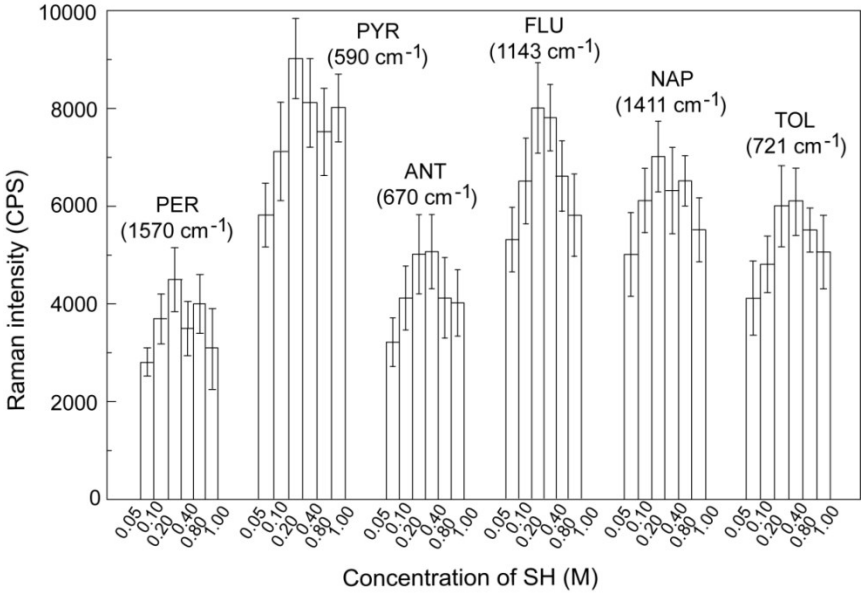

Fig. S14 The representative vibration peaks of PAHs as a function of SH (hexanethiol) concentration. Each data point represents the average value from five SERS spectra on each sample. Error bars show the standard deviations associated with five measurements.

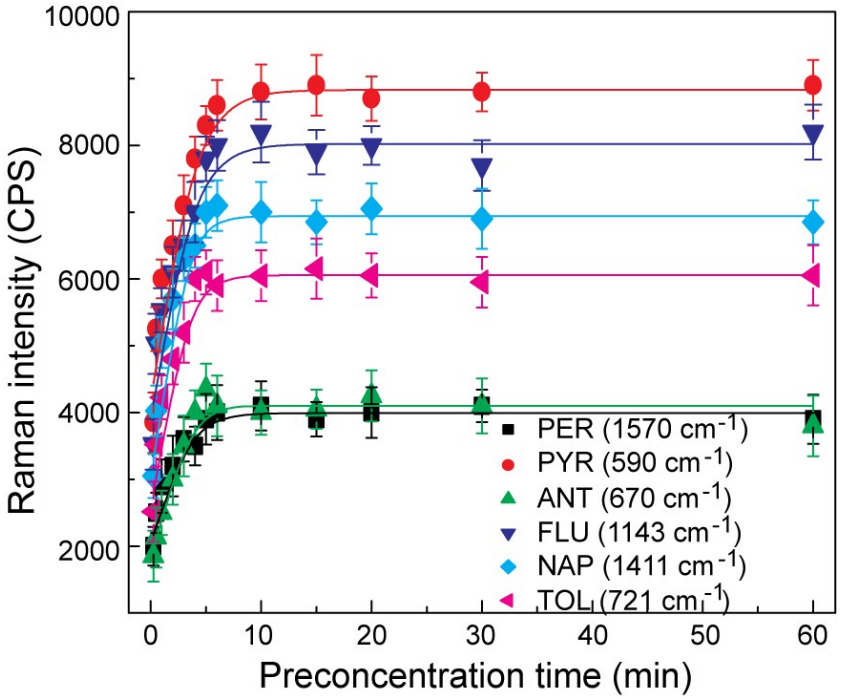

Fig. S15 The SERS signals of representative vibration peaks of PAHs on Ag/GN-SH increased with preconcentration time. The SERS intensity of PAHs reached saturation limit about after 5 min. The concentration of TOL, NAP, ANT, FLU, PYR and PER for detection is 3×10^{-5} M, 8×10^{-7} M, 2×10^{-6} M, 1×10^{-6} M, 2×10^{-6} M and 5×10^{-6} M, respectively.

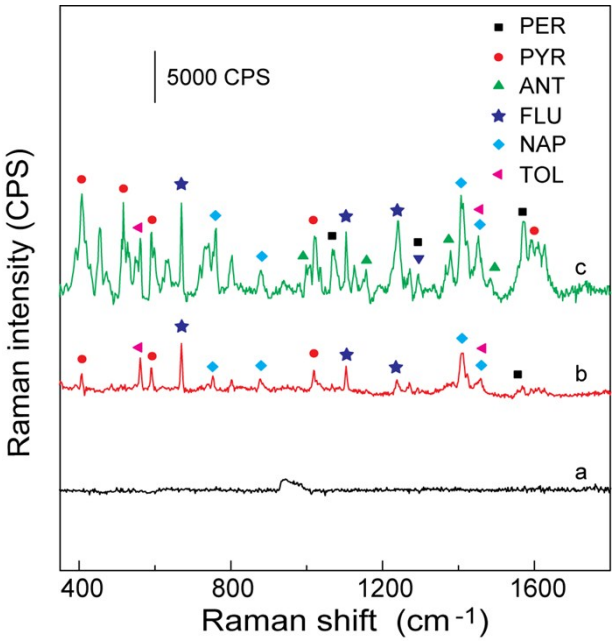

Fig. S16 (a) The SERS spectrum of PAHs extracted directly from the tap water samples; the SERS spectrum of the extract in the presence of six PAHs at the concentration (b) 0.1 M and (c) 1.0 M, respectively.

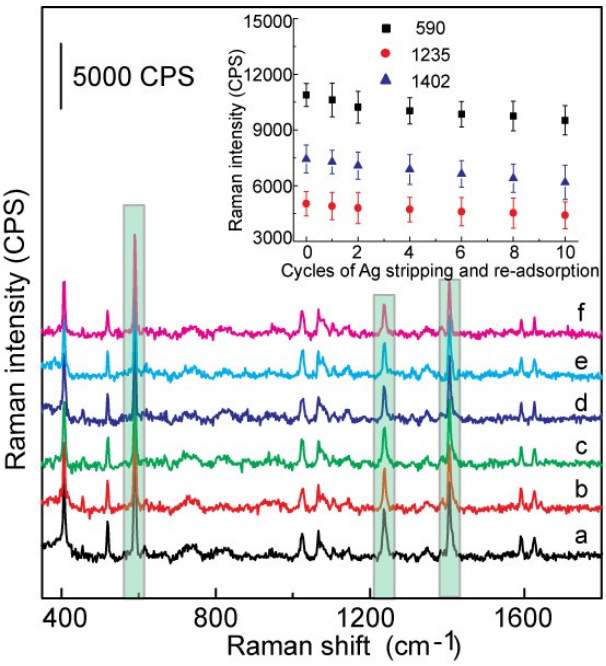

Fig. S17 SERS spectra investigation of the recyclability of Ag/GN-SH after 1~10 stripping and re-adsorption of Ag NPs. SERS spectra of Ag/GN-SH after incubating with 2×10^{-6} M PYR for 5 min. A fresh prepared Ag/GN-SH (a), after 1 (b), 3 (c), 5 (d), 8 (e) and 10 (f) stripping and re-adsorption of Ag cycle. The inset shows the representative vibration peaks of PYR variation with cycles of Ag stripping and re-adsorption, respectively. Each data point represents the average value from five SERS spectra on each sample. The error bars represent typical intensity variations obtained from the same sample measured at five different spots.

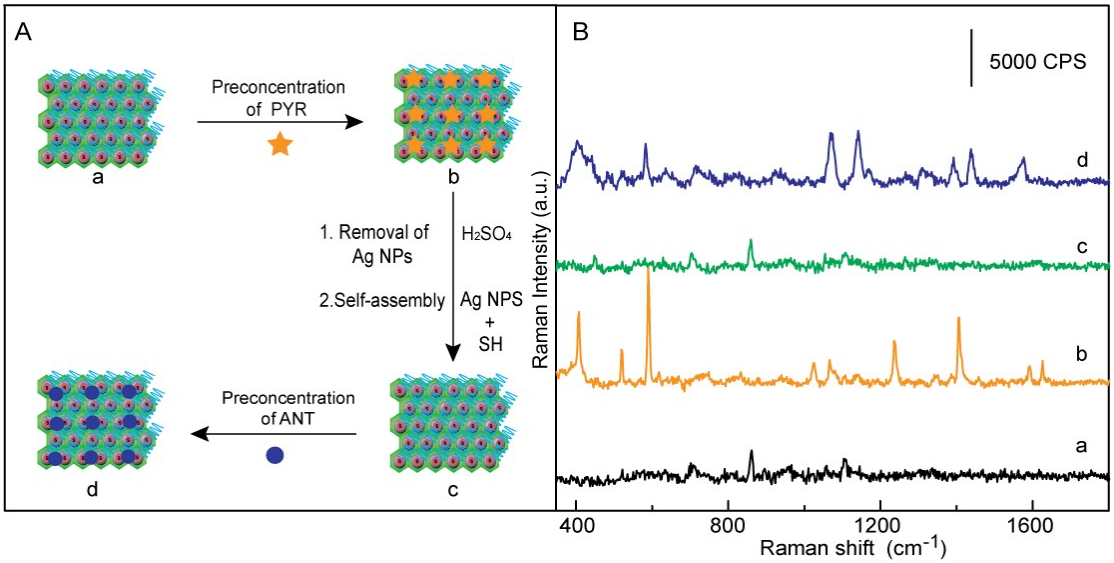

Fig. S18 (A) Schematic representation of Ag/GN-SH can be reused as SERS substrates. (B) Raman spectra of Ag/GN-SH substrate (a), SERS spectrum of Ag/GN-SH in the solution containing 2×10^{-6} M PYR for 5 min (b), then the Ag/GN-SH were stripped off and followed by assembly of Ag NPs (c) and treated with the 2×10^{-6} M

ANT for 5 min (d).

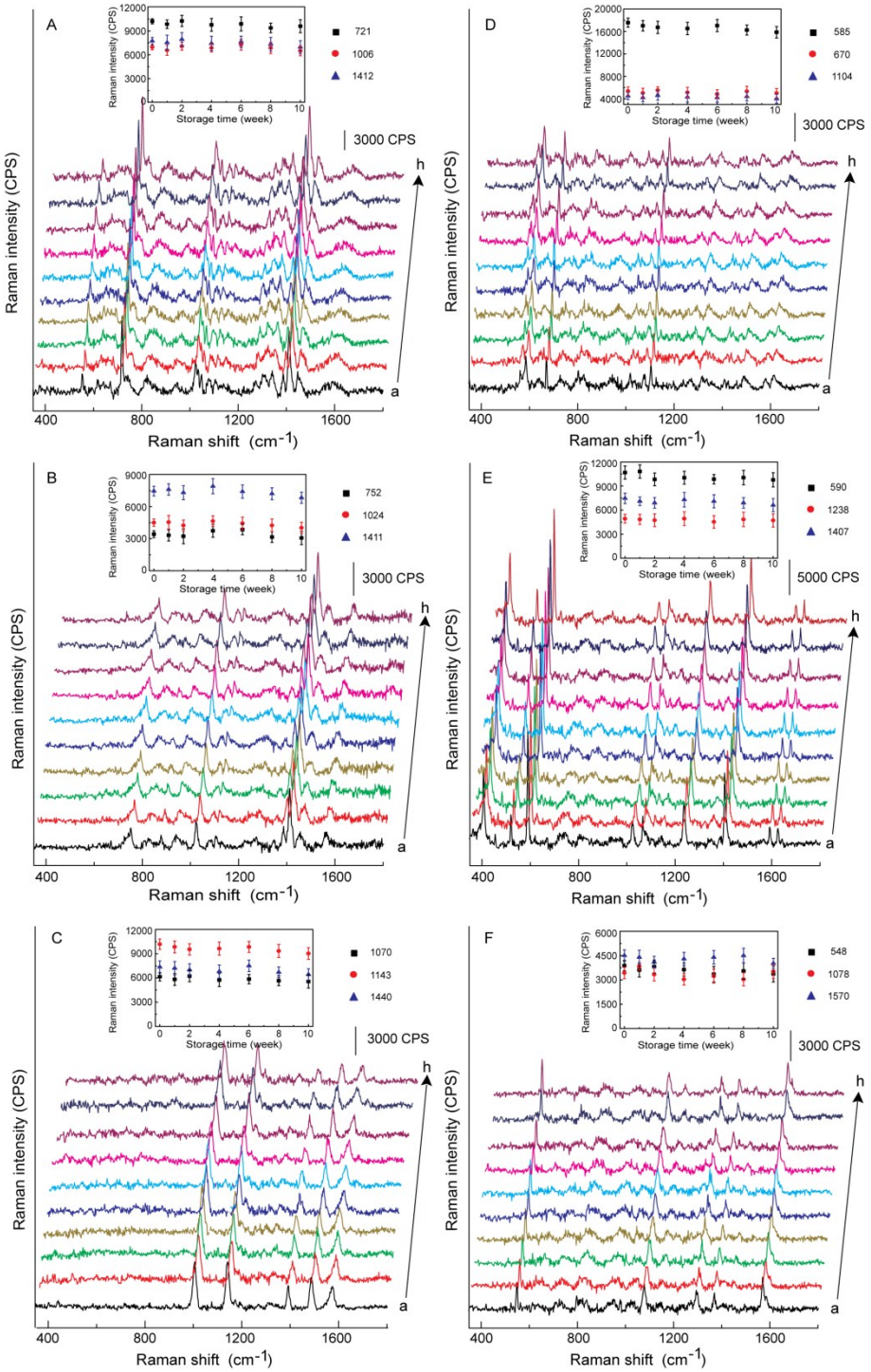

Fig. S19 The stability of the SERS signal on the Ag/GN-SH. SERS spectra of (A) toluene, (B) naphthalene, (C) anthracene, (D) fluoranthene, (E) pyrene and (F) perylene on the Ag/GN-SH stored from one to ten weeks (from a to h) under ambient conditions. The concentration of (A−F) for detection is 3×10^{-5} M, 8×10^{-7} M, 2×10^{-6} M, 1×10^{-6} M, 2×10^{-6} M and 5×10^{-6} M. All SERS spectra have been baseline-corrected. Inset: SERS intensity distribution of the representative vibration peaks of the analytes plotted against time. Each data point represents the average value from five SERS

spectra. Error bars show the standard deviations.

Table S1 Results of fitting Langmuir, Freundlich, and DA models to the adsorption data of PAHs on Ag/GN-SH.

Samples	Langmuir			Freundlich			DA		
	Q_m (μg/mg)	K_L (L/g)	R^2	K_F [(mg/g)/(mg/L)^n]	1/n	R^2	Q_m (μg/mg)	E (kJ/mol)	R^2
PER	198.3	201.8	0.988	288.5	0.263	0.991	253.3	21.35	0.999
PYR	164.8	229.2	0.968	253.8	0.285	0.998	201.4	19.04	0.998
ANT	115.2	274.7	0.978	207.1	0.311	0.978	155.1	15.14	0.999
FLU	88.7	312.5	0.965	168.3	0.298	0.968	103.5	12.35	0.998
NAP	63.6	334.9	0.966	122.4	0.336	0.988	80.4	10.25	0.999
TOL	35.4	389.1	0.962	85.3	0.358	0.992	48.2	13.18	0.999

Table S2 Physical Properties of the GO, Cys-GN and Ag/GN-SH.

Samples	BET surface area ($m^2 g^{-1}$) [a]	Total pore volume ($cm^3 g^{-1}$) [b]	Pore diamater (nm) [c]
GO	55	0.08	20.5
Cys-GN	325	1.06	12.3
Ag/GN-SH	530	1.83	10.2

a BET surface area calculated from the nitrogen adsorption isotherm using the BET method.

b Total pore volume at P/P0 = 0.97.

c Data obtained from Barret−Joyner−Halenda (BJH) desorption average pore diameter.

Table S3 Experimental Raman shifts (cm^{-1}) of methyl violet (MV).

Raman (cm^{-1}) [a]	SERS (cm^{-1})	Assignment	Raman Ref.
398(m)	400(s)	N-CH_3 ip def.	400
411(s)		N-CH_3 ip def.	410
654(m)	660(s)	C-C ring ip def.	660
686(m)	692(m)	C-C ring ip def.	685
840(s)	837(vs)	C-C ring op def.	842
1197(s)	1191(s)	N-CH_3 str.	1194
1302(s)	1295(s)	C-C ring str.	1302
1653(m)	1649(vs)	C-C ring str.	1657

[a] Abbreviations used: w, weak; m, medium; s, strong; vs, very strong; str., stretching; def., deformation; ip, in-plane; op, out-of-plane. Wavenumber is given in cm^{-1}

Table S4 Experimental Raman shifts (cm^{-1}) of toluene (TOL)

Raman (cm^{-1}) [a]	SERS (cm^{-1})	Assignment	Raman Ref.
560(vw)	557(m)	C-C ring def.	560
617(w)	618(s)	C-C ring def.	606
679(w)		CH_3 bend	673
711(vw)	720(s)	C-C ring def.	703
1005(s)	1008(m)	C-C ring str.	1010
1034(m)	1035(m)	CH_3 op def.	1041
1417(vw)	1412(s)	CH_3 ip def.	1436
1450(vw)	1455(m)	C-C ring str.	1448

[a] Abbreviations used: w, weak; m, medium; s, strong; vs, very strong; str., stretching; def., deformation; ip, in-plane; op, out-of-plane. Wavenumber is given in cm^{-1}

Table S5 Experimental Raman shifts (cm^{-1}) of naphthalene (NAP)

Raman (cm^{-1}) [a]	SERS (cm^{-1})	Assignment	Raman Ref.
760(vs)	754(m)	C-H op def.	761
870(vw)	877(m)	C-H op def.	886
1020(s)	1025(m)	C-C ring str.	1020
1381(vs)	1385(m)	Ring ip def.	1382
1400(vw)	1412(s)	Ring ip def.	1405
1464(m)	1457(m)	C-C ring str. + C-C ip def.	1464
1577(m)	1566(m)	C-C ring str.	1577
1630(w)		C-C ring str.	1464

[a] Abbreviations used: w, weak; m, medium; s, strong; vs, very strong; str., stretching; def., deformation; ip, in-plane; op, out-of-plane. Wavenumber is given in cm^{-1}

Table S6 Experimental Raman shifts (cm^{-1}) of anthracene (ANT)

Raman (cm^{-1}) [a]	SERS (cm^{-1})	Assignment	Raman Ref.
396(s)		Skeletal deformation	394
756(s)		C-C ring str.	753
1007(w)	1005(s)	C-C ring str.	1008
1163(w)	1143(vs)	C-C ring str.	1165
1186(w)	1193(m)	C-C ring str.	1188
1403(s)	1391(s)	C-C ring str.	1403
1482(w)	1485(s)	C-C ring str.	1482
1559(w)	1577(m)	C-C ring str.	1560

[a] Abbreviations used: w, weak; m, medium; s, strong; vs, very strong; str., stretching; def., deformation; ip, in-plane; op, out-of-plane. Wavenumber is given in cm^{-1}

Table S7 Experimental Raman shifts (cm^{-1}) of fluoranthene (FLU)

Raman (cm^{-1}) [a]	SERS (cm^{-1})	Assignment	Raman Ref.
470(w)		Skeletal str.	470
567(m)	578(vs)	Skeletal str.	563
670(s)	669(m)	C-H str.	665
802(w)	800(w)	C-H str.	795
1019(m)	1018(w)	C-C str.	1013
1103(s)	1105(m)	C-H ip def.	1097
1269(w)	1259(w)	C-H ip def.	1262
1411(m)	1408(w)	Ring str.	1406
1421(m)	1423(w)	C-C str.	1414
1454(w)	1451(w)	C-C str.	1450
1610(s)	1613(m)	C-C str.	1605

[a] Abbreviations used: w, weak; m, medium; s, strong; vs, very strong; str., stretching; def., deformation; ip, in-plane; op, out-of-plane. Wavenumber is given in cm^{-1}

Table S8 Experimental Raman shifts (cm^{-1}) of pyrene (PYR)

Raman (cm^{-1}) [a]	SERS (cm^{-1})	Assignment	Raman Ref.
406(s)	409(s)	Skeletal str.	410
455(w)	455(w)	Skeletal str.	456
505(w)	521(m)	Skeletal def.	512
592(s)	590(vs)	Skeletal str.	594
1065(m)	1067(m)	C-H ip def.	1068
1143(w)	1135(w)	C-H ip def.	1144
1242(s)	1238(s)	C-H ip def.	1241
1406(s)	1408(s)	C-C str.	1408
1551(m)	1560(w)	C-C str.	1552
1594(m)	1590(m)	C-C str.	1596
1628(m)	1624(m)	C-C str.	1626
1645(w)	1642(w)	C-C str.	1640

[a] Abbreviations used: w, weak; m, medium; s, strong; vs, very strong; str., stretching; def., deformation; ip, in-plane; op, out-of-plane. Wavenumber is given in cm^{-1}

Table S9 Experimental Raman shifts (cm^{-1}) of perylene (PER)

Raman (cm^{-1}) [a]	SERS (cm^{-1})	Assignment	Raman Ref.
531(w)	522(s)	C-C-C-H op def.	538
549(s)	550(m)	C-C-C def.	550
842(s)	838(w)	C-C str. + C-H ip def.	850
979(s)	976(w)	C-C str.	980
1070(w)	1075(m)	C-C-C-H op def.	1076
1140(m)	1145(s)	C-H ip def.	1408
1299(s)	1294(m)	C-C str.	1296
1374(s)	1367(m)	C-C str.	1373
1571(s)	1568(m)	C-C str.	1571

[a] Abbreviations used: w, weak; m, medium; s, strong; vs, very strong; str., stretching; def., deformation; ip, in-plane; op, out-of-plane. Wavenumber is given in cm^{-1}

References:

1 E. C. Le Ru, E. Blackie, M. Meyer and P. G. Etchegoin, *J. Phys. Chem. C*, 2007, **111**, 13794-13803.

2 A. D. McFarland, M. A. Young, J. A. Dieringer and R. P. Van Duyne, *J. Phys. Chem. B*, 2005, **109**, 11279-11285.

3 D. Li, D. W. Li, Y. Li, J. S. Fossey and Y. T. Long, *J. Mater. Chem.*, 2010, **20**, 3688-3693.

4 Z. T. Deng, H. Lin, W. Ji, L. Gao, X. Lin, Z. H. Cheng, X. B. He, J. L. Lu, D. X. Shi, W. A. Hofer and H. J. Gao, *Phys. Rev. Lett.*, 2006, **96**, 156102.

5 J. Wang, Z. M. Chen and B. L. Chen, *Environ. Sci. Technol.*, 2014, **48**, 4817-4825.

6 Y. B. Sun, S. B. Yang, G. X. Zhao, Q. Wang and X. K. Wang, *Chem. Asian J.*, 2013, **8**, 2755-2761.